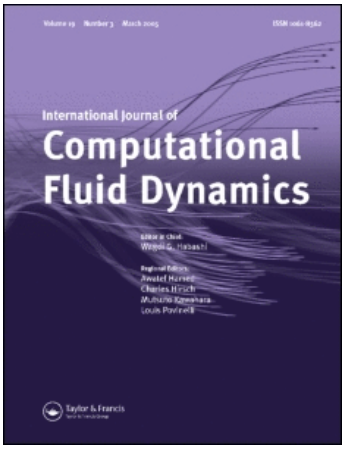

International Journal of Computational Fluid Dynamics
Publication details, including instructions for authors and subscription information:
http://www.informaworld.com/smpp/title~content=t713455064

Validation of hyperbolic model for two-phase flow in conservative form

D. Zeidan [a]; A. Slaouti [b]
[a] Department of Applied Sciences, Al-Balqa Applied University, Al-Salt, Jordan [b] Department of Engineering and Technology, Manchester Metropolitan University, Manchester, UK

Online publication date: 04 December 2009

To cite this Article Zeidan, D. and Slaouti, A.(2009) 'Validation of hyperbolic model for two-phase flow in conservative form', International Journal of Computational Fluid Dynamics, 23: 9, 623 — 641
To link to this Article: DOI: 10.1080/10618560903367759
URL: http://dx.doi.org/10.1080/10618560903367759

International Journal of Computational Fluid Dynamics
Vol. 23, No. 9, October–November 2009, 623–641

Taylor & Francis
Taylor & Francis Group

Validation of hyperbolic model for two-phase flow in conservative form

D. Zeidan[a]* and A. Slaouti[b]

[a]*Department of Applied Sciences, Al-Balqa Applied University, Al-Salt, Jordan;* [b]*Department of Engineering and Technology, Manchester Metropolitan University, Manchester, UK*

(*Received 12 June 2009; final version received 24 September 2009*)

A mathematical formulation is proposed for the solution of equations governing isentropic gas–liquid flow. The model considered here is a two-fluid model type where the relative velocity between the two phases is implemented by a kinetic constitutive equation. Starting from the conservation of mass and momentum laws, a system of three differential equations is derived in a conservative form for the three principal variables, which are mixture density, mixture velocity and the relative velocity. The governing equations for the mixture offer the novel hyperbolic conservation laws for the description of two-phase flows without any conventional source terms in the momentum or relative velocity equations. The discretisation of the governing equations is based on splitting approach, which is specially designed to allow a straightforward extension to various numerical methods such as Godunov methods of centred-type. To verify the validity of the model, numerical results are presented and discussed. It is demonstrated that the proposed numerical methods have superior overall numerical accuracy among existing methods and models in the literature. The model correctly describes the formation of shocks and rarefactions for the solution of discontinuities in two-phase fluid flow problems, thus verifying the proposed mathematical and numerical investigations.

Keywords: two-phase flows; fully conservative approach; hyperbolic PDEs; finite volumes; Godunov centred methods

1. Introduction

Two-phase flows occur in many scientific and technical disciplines ranging from natural and man-made processes to the modelling of normal operation or accident conditions in nuclear, petroleum or process engineering installations. Understanding and accurately modelling such flows lead to greatly improved designs of two-phase flow problems in an established process. For a long time, the analysis of these flows was restricted to typically empirical correlations or to largely simplified engineering models. In recent decades, considerable attention has been spent for the mathematical modelling and for the numerical treatment of two-phase flows. This interest caused by the specific requirements provides a productive problem solving environment for the researchers in this field. It has been well known that the differential equation systems modelling the two-phase flows pose enormous challenges for steady state solution. For instance, the mathematical equations of two-phase flows have a rich and complex structure. The structure is often very sensitive to the character of the equations. The substantial body of available two-phase flow equations is based on averaging the instantaneous local equations of motion along with closure relations. In general, the closure relations are formulated in terms of averaged variables and are specific to the structure of the flow where they have to be separately supplied for each flow pattern (Delhaye and Achard 1976, Nigmatulin 1979, Drew 1983, Baer and Nunziato 1986, Brennen 2005). Models for two-phase flows can be categorised in two different classes (Ishii 1975): two-fluid models and mixture models (diffusion models). In the two-fluid models, which is the model under consideration in the present work, the equations are written for mass, momentum and energy balances for each phase separately. In contrast, the mixture models treats the two phases as a mixture where the equations for conservation of physical properties are written for the two-phase mixture. The two-fluid models for two-phase flows presents more general and detailed solution compared to mixture models. However, more closure models are required with the two-fluid models whereas mixture models have a reduced number of balance equations. Two essential characteristics have emerged for two-phase flow models. The first one is related to the character type of the governing equations (hyperbolic or non-hyperbolic). Clearly, hyperbolicity is an essential requirement for well-posedness of the problem (Stewart and Wendroff 1984). The second characteristic concerns the possibility of expression of the governing equations in

*Corresponding author. Email: dia@bau.edu.jo

ISSN 1061-8562 print/ISSN 1029-0257 online

DOI: 10.1080/10618560903367759
http://www.informaworld.com

conservation-law form. That is, whether the equations have, or have not, the conservative character in the mathematical sense. Non-conservative formulation is a serious mathematical difficulty as one cannot define discontinuous solutions such as shock waves and associated Rankine-Hugoniot conditions (Serre 1993, Gouin and Gavrilyuk 1999). It has been recognised that non-hyperbolicity and non-conservative form of the governing equations are major reasons for causing mathematical and numerical difficulties. A number of attempts have been made to improve the mathematical properties of the two-phase flow equations. More physical effects, such as the virtual mass (Drew *et al*. 1979, Toumi and Kumbaro 1996), the interfacial pressure terms (Stuhmiller 1977, Sha and Soo 1979) and the surface tension force terms (Lee *et al*. 1998) can be more correctly modelled in order to make the equations hyperbolic. A different approach has been to consider mixture formulation for the flow models of interest, see for instance (Bdzil *et al*. 1999, Papalexandris 2004). Yet, most of these models have a non-conservative form because of the interface interaction. More recently, another interesting approach to model two-phase flows is based on the formulation of thermodynamically compatible systems (Godunov and Romenskii 2003). This results in a fully conservative hyperbolic model in terms of parameters of state for the mixture (Romenski *et al*. 2007, Zeidan *et al*. 2007a). Because of the progress in the development of two-phase flow models, there has been also progress in the construction of numerical methods for solving these models. Some typical examples, the commercial codes such as CATHARE (Barre and Bernard 1986), OLGA (Bendiksen *et al*. 1991), Petra (Larsen *et al*. 1997) and RELAP (Shieh *et al*. 1994) are known to be robust but too diffusive (Toumi 1996). A variety of upwind methods have been proposed for solving two-phase flow models as well. Many of these methods are regarded as flux vector splitting (FVS) methods (Chung *et al*. 2002, Stadtke 2006) and flux difference splitting (FDS) methods (Tiselj and Petelin 1997, Romate 1998). The AUSM method family has also been implemented successfully to two-phase flows (Niu 2001, Paillere *et al*. 2003). Recently, Godunov methods of upwind and centred type have been applied for solving two-phase flow models, provided that the equations system is hyperbolic. Such methods are very efficient, accurate and robust. Examples for such methods for two-phase flow models, two-fluid models as well as mixture models are proposed by Garcia-Cascales and Corberin-Salvador (2006), Castro and Toro (2006), Coquel *et al*. (1997), Masella *et al*. (1999), Romenski and Toro (2004), Zeidan (2005).

The aim of this article is to propose a simple and hyperbolic two-fluid model for the best description of two-phase flows. In particular, the model proposed here is a fully conservative, physically reliable and independent of the kind of numerical method used to implement it and produce oscillation-free solutions of discontinuities in two-phase flow problems. The model describes a one-dimensional isentropic gas–liquid two-phase flow with a velocity difference between the two phases. The system of equations is based on mass and momentum equations for the two phases under a common pressure field. These isentropic four equations are of non-conservative form and they are ill-posed in the sense that the eigenvalues are complex. Thus, the isentropic four equations contain the essential features for our purpose. The isentropic four equations are used in this article as the basis for deriving the hyperbolic conservative two-phase flow equations in a mixture form. The mixture formulation provides an alternative approach to the problem. In this approach, both the continuity equation and momentum equation are written for the mixture of gas–liquid phases. The momentum equation can also be written in a different formulation in which the relative velocity between phases can be expressed by a constitutive equation. Therefore, the two-phase flow model equations consists of a mixture of mass and momentum conservation equations and of an equation for the relative velocity between the two phases in a conservative form. Moreover, these three equations offer a novel and fully conservative hyperbolic system of governing equations that can be used for the description of two-phase flows and that can be implemented and solved by any type of numerical methods. Considering only the numerical aspect of the present work, the numerical method employed for solving the model equations is not important. Though any kind of numerical methods applicable for the solution of hyperbolic conservation laws can be used (see e.g. Collela and Woodward 1984, Harten 1989, Ren *et al*. 1996, Toro 2009), here we intend to adapt Godunov methods based on operator splitting approach (Strang 1968) to approximate solutions of the proposed system of governing equations. The splitting procedure separate the model equations into two problems: a homogeneous problem in which no sources are included and a second problem with the source terms only. This strategy enables the use of separate solvers for both the homogeneous problem in which discontinuities are present and for the non-homogeneous problem in which phase-interaction occurs through the source terms. We have chosen Godunov methods because they have been specifically developed to provide high accuracy while avoiding the numerical diffusion (i.e. smearing) and numerical dispersion (i.e. non-physical

oscillations) associated with other finite difference and finite volume methods.

The model equations are described in section 2. We focus on the assumptions made which lead to conservative two-phase flow equations. In section 3, the mathematical properties of the equations are introduced and the model equations are rewritten in an equivalent form. The Jacobian matrix of the model is derived and results on the hyperbolicity of the model are presented under the assumption that the relative velocity between the two phases is much lower than the speed of sound of the two-phase mixture. In section 4, we investigate the nature of characteristic fields associated with the eigenstructure of the model equations. We show that the first and third characteristic fields are genuinely non-linear while the second characteristic field is neither genuinely non-linear nor linearly degenerate. The proposed numerical methods for solving the governing equations are briefly described in section 5, and this is followed in section 6 with a presentation of the numerical results. The analysis of these results and comparison with the results obtained with other two-phase flow models are also presented in this section. The final section of the article gives conclusions and closing remarks.

2. The governing equations

In this section, we study the two-phase flow averaged equations (Ishii 1975, Lahey and Drew 1988) that have been obtained as a result of time, space or ensemble averaging of the instantaneous local balance equations. For brevity and without loss of generality, the simplest two-fluid model proposed in the literature (see e.g. Drew and Passman 1998) is considered. In this model, the equations govern the dynamics of two fluids (called phases, hereafter), such as liquid and gas. These equations in the case of a one-dimensional inviscid two-phase flow are given by two mass and two momentum balance equations for each phase in the following way:

$$\partial_t(\alpha_2\rho_2) + \partial_x(\alpha_2\rho_2 u_2) = \overline{\mathcal{S}}_2, \tag{1}$$

$$\partial_t(\alpha_1\rho_1) + \partial_x(\alpha_1\rho_1 u_1) = \overline{\mathcal{S}}_1, \tag{2}$$

$$\partial_t(\alpha_2\rho_2 u_2) + \partial_x(\alpha_2\rho_2 u_2^2) + \alpha_2\partial_x P = \mathcal{S}_2, \tag{3}$$

$$\partial_t(\alpha_1\rho_1 u_1) + \partial_x(\alpha_1\rho_1 u_1^2) + \alpha_1\partial_x P = \mathcal{S}_1. \tag{4}$$

Isentropic conditions are assumed within the equations (no energy balance is needed). Index 1 is referred to the liquid and index 2 to the gas phase; t is the time and x is the space coordinate; ρ_j and u_j are the density and velocity of phase j ($j = 1, 2$); P is the pressure common to both phases and calculated as

$$P = K\rho_2^{\gamma}, \tag{5}$$

where ρ_2 is the gas phase density, K is assumed to be a known constant and γ is the usual ratio of specific heats, which we regard as being given. Finally, α_j is the volume fraction of phase j related by

$$\alpha_1 + \alpha_2 = 1, \tag{6}$$

which closes the system of the equations.

The source terms on the right-hand sides of the governing equations consists of constitutive relations for the interface transfers with an algebraic expression. We prefer source terms of algebraic form because they will not alter the mathematical property of the above differential equations system. For the purposes of this article, we have the following relations at the interface:

$$\overline{\mathcal{S}}_2 + \overline{\mathcal{S}}_1 = 0,$$

that is no mass transfer between phases. The momentum source terms $\mathcal{S}_2$ and $\mathcal{S}_1$ models the interaction between the phases:

$$\mathcal{S}_2 + \mathcal{S}_1 = 0,$$

with

$$\mathcal{S}_j = B_j + \mathcal{S}_j^I + \mathcal{S}_j^{\mathrm{w}} + \mathcal{S}_j^{\mathrm{vm}} + \mathcal{S}_j^P$$

for the j-phase,

where $\mathcal{S}_j^P$ denotes the pressure default $P - P_j$ between the bulk average pressure and the interfacial average pressure, $\mathcal{S}_j^{\mathrm{vm}}$ stands for the virtual mass force and $\mathcal{S}_j^{\mathrm{w}}$ represents the wall frictional force for the j-phase. $\mathcal{S}_j^I$and B_j denote the interaction between phases and the gravitational force, respectively. The gravitational force that will be considered here is the gravity:

$$B_j = \alpha_j\rho_j g_x, \tag{7}$$

where $g_x = g$ is the acceleration of the gravity in the x direction. In addition, the exchange of momentum between phases is due to the drag force which is the most common interphase force (Ishii and Zuber 1979). The main objective here is not to consider all these aspects but rather specify some simple models that can used for the mathematical and numerical investigations. Thus, the momentum Equations (3) and (4) can be written as

$$\partial_t(\alpha_2\rho_2 u_2) + \partial_x(\alpha_2\rho_2 u_2^2) + \alpha_2\partial_x P = \alpha_2\rho_2 g - \mathcal{S}^I, \tag{8}$$

$$\partial_t(\alpha_1\rho_1 u_1) + \partial_x(\alpha_1\rho_1 u_1^2) + \alpha_1\partial_x P = \alpha_1\rho_1 g + \mathcal{S}^I. \tag{9}$$

Here $\mathcal{S}^I = \mathcal{S}^I_j$ models the interaction between the phases through the drag force

$$\mathcal{S}^I = \kappa(u_2 - u_1), \tag{10}$$

where κ is a positive parameter or function.

System (1)–(4) is not written in standard conservation form because of the presence of non-conservative product $\alpha_j \partial_x P$ in the phase momentum equations. It is necessary, therefore, to rewrite these equations in a suitable form for mathematical investigations. This could be accomplished as follows. A total mass conservation equation is obtained by adding Equations (1) and (2) giving

$$\partial_t(\alpha_2\rho_2 + \alpha_1\rho_1) + \partial_x(\alpha_2\rho_2 u_2 + \alpha_1\rho_1 u_1) = 0. \tag{11}$$

The momentum equation is written in sum and difference form. Thus, a total momentum equation is obtained by adding Equation (3) and (4), or Equations (8) and (9), giving

$$\partial_t(\alpha_2\rho_2 u_2 + \alpha_1\rho_1 u_1) + \partial_x(\alpha_2\rho_2 u_2^2 + \alpha_1\rho_1 u_1^2) + \partial_x P = (\alpha_2\rho_2 + \alpha_1\rho_1)g. \tag{12}$$

The two momentum Equations (3) and (4), or (8) and (9), are combined by dividing the liquid phase momentum equation by $\alpha_1\rho_1$ and the gas phase momentum equation by $\alpha_2\rho_2$ then taking the difference leading to

$$\partial_t(u_2 - u_1) + \partial_x\left(\frac{u_2^2}{2} - \frac{u_1^2}{2}\right) + \partial_x\psi(P) = -\mathcal{S}^I\left(\frac{1}{\alpha_2\rho_2} + \frac{1}{\alpha_1\rho_1}\right), \tag{13}$$

where

$$\psi(P) = \frac{\gamma}{\gamma - 1}\rho_2^{-1}P - \frac{P}{\rho_1}. \tag{14}$$

Therefore, we have reduced the original isentropic non-conservative four Equations (1)–(4) to the following three differential equations

$$\partial_t(\alpha_2\rho_2 + \alpha_1\rho_1) + \partial_x(\alpha_2\rho_2 u_2 + \alpha_1\rho_1 u_1) = 0, \tag{15}$$

$$\partial_t(\alpha_2\rho_2 u_2 + \alpha_1\rho_1 u_1) + \partial_x(\alpha_2\rho_2 u_2^2 + \alpha_1\rho_1 u_1^2) + \partial_x P = (\alpha_2\rho_2 + \alpha_1\rho_1)g, \tag{16}$$

$$\partial_t(u_2 - u_1) + \partial_x\left(\frac{u_2^2}{2} - \frac{u_1^2}{2}\right) + \partial_x\psi(P) = -\mathcal{S}^I\left(\frac{1}{\alpha_2\rho_2} + \frac{1}{\alpha_1\rho_1}\right), \tag{17}$$

which form a simplified version of system (1)–(4). Systems (15)–(17) suggest the mixture quantities

$$\rho = \alpha_2\rho_2 + \alpha_1\rho_1, \tag{18}$$

$$\rho u = \alpha_2\rho_2 u_2 + \alpha_1\rho_1 u_1, \tag{19}$$

$$c = \frac{\alpha_2\rho_2}{\rho}. \tag{20}$$

If we use Equation (20) in Equation (18), then the mixture density ρ may be defined by

$$\frac{1}{\rho} = \frac{c}{\rho_2} + \frac{1-c}{\rho_1}. \tag{21}$$

It follows from Equations (5), (20) and (21) that

$$\rho = \rho(P), \tag{22}$$

which is the generalised equation of state in a mixture formulation. Finally, a hydrodynamical closure relating the two-phase velocities is implemented by a kinetic constitutive equation such as

$$u_r = u_2 - u_1. \tag{23}$$

Closing system (15)–(17) with the standard relations (18)–(23), the final working equations are

$$\partial_t(\rho) + \partial_x(\rho u) = 0, \tag{24}$$

$$\partial_t(\rho u) + \partial_x(\rho u^2 + \rho c(1-c)u_r^2) + \partial_x P = \rho g, \tag{25}$$

$$\partial_t(u_r) + \partial_x\left(uu_r + (1-2c)\frac{u_r^2}{2}\right) + \partial_x\psi(P) = \frac{-\mathcal{S}^I}{\rho c(1-c)}. \tag{26}$$

This set of equations written in terms of the mixture parameters in a conservative form will be referred to henceforth as the working model for one-dimensional isentropic gas–liquid mixture flow. Equations (24)–(26) are the balance laws for mixture mass, mixture momentum and relative velocity, respectively, in a conservative form.

3. Hyperbolicity analysis of the equations

The system of differential Equations (24)–(26) corresponding to the isentropic gas–liquid mixture

two-phase flow is equivalent to the following conservative form

$$\partial_t \mathbb{U} + \partial_x \mathbb{F}(\mathbb{U}) = \mathbb{S}(\mathbb{U}), \tag{27}$$

with $t \in \mathbb{R}^+$, $x \in \mathbb{R}$, $\mathbb{U}(x, t) \in \mathbb{R}^3$, and $\mathbb{F}:\mathbb{R}^3 \to \mathbb{R}^3$ a smooth map ($\mathbb{R}^3$ is the set of real numbers) and $\mathbb{U}$, $\mathbb{F}(\mathbb{U})$, $\mathbb{S}(\mathbb{U})$ are the conservative variables, the conservative fluxes and the source terms, respectively, given by

$$\mathbb{U} = \begin{pmatrix} \rho \\ \rho u \\ u_r \end{pmatrix}, \quad \mathbb{F}(\mathbb{U}) = \begin{pmatrix} \rho u \\ \rho u^2 + P + \rho c(1-c)u_r^2 \\ u u_r + (1-2c)\frac{u_r^2}{2} + \psi(P) \end{pmatrix},$$

$$\mathbb{S}(\mathbb{U}) = \begin{pmatrix} 0 \\ \rho g \\ \frac{-\mathcal{S}^I}{\rho c(1-c)} \end{pmatrix}. \tag{28}$$

The inhomogeneous conservation laws (27) may also be written in quasi-linear form

$$\partial_t \mathbb{U} + \mathbb{J}\partial_x(\mathbb{U}) = \mathbb{S}(\mathbb{U}), \tag{29}$$

where $\mathbb{J}$ is the Jacobian matrix of $\mathbb{F}$ with respect to the conservative variables $\mathbb{U}$.

In general, it is difficult to express the flux function $\mathbb{F}$ in terms of conservative variables specially when considering two-phase fluid flow problems. Furthermore, to determine the classification of the model equations and to provide the mathematical framework needed for the development of numerical methods, we formulate the model Equations (24)–(26) using a set of generic variables $\mathbb{W}$ instead of the conserved variables $\mathbb{U}$. An alternative choice of variables, and formulation, is normally referred to as primitive variables (Thomas and Lombard 1979), and is usually denoted as $\mathbb{W}$:

$$\mathbb{W} = [\rho, u, u_r]^T, \tag{30}$$

Thus, we rewrite the governing equations in the form

$$\mathbb{C}(\mathbb{W})\partial_t \mathbb{W} + \mathbb{A}(\mathbb{W})\partial_x \mathbb{W} = \mathbb{Q}(\mathbb{W}), \tag{31}$$

where the coefficient matrices are defined as

$$\mathbb{C}(\mathbb{W}) = \begin{pmatrix} a_m^{-2} & 0 & 0 \\ 0 & \rho & 0 \\ 0 & 0 & 1 \end{pmatrix}, \tag{32}$$

$$\mathbb{A}(\mathbb{W}) = \begin{pmatrix} \frac{u}{a_m^2} & \rho & 0 \\ 1 + c(1-c)\frac{u_r^2}{a_m^2} + (1-2c)\frac{\partial c}{\partial P}\rho u_r^2 & \rho u & 2\rho c(1-c)u_r \\ \frac{\partial \psi}{\partial P} - \frac{\partial c}{\partial P}u_r^2 & u_r & u + (1+2c)u_r \end{pmatrix}, \tag{33}$$

and $\mathbb{Q}(\mathbb{W}) = \frac{\partial \mathbb{W}}{\partial \mathbb{U}}\mathbb{S}(\mathbb{U})$.

To examine the hyperbolicity of the simplest form of two-fluid models, we assume that the relative velocity, u_r, between phases is much lower than the speed of sound, a_m. Such an assumption arise in the modelling of many physical systems such as pipelines (see e.g. Toumi and Kumbaro 1996, Lee *et al.* 1998, Romenski and Toro 2004, Baudin *et al.* 2005, Zeidan *et al.* 2007a). Thus, we will introduce a small parameter, η, given by

$$\eta = \frac{u_r}{a_m} = \frac{u_2 - u_1}{a_m} \ll 1, \tag{34}$$

where a_m defined as

$$a_m = \left(\frac{\partial P}{\partial \rho}\right)^{\frac{1}{2}}. \tag{35}$$

We also assume that the following relations are satisfied

$$\frac{\partial P}{\partial \rho} > 0, \quad 2\frac{\partial P}{\partial \rho} + \rho\frac{\partial^2 P}{\partial \rho^2} > 0, \tag{36}$$

to ensure that the pressure P is a convex function of the specific volume $\frac{1}{\rho}$. Further, for the generalised isentropic equation of state (22), the system (27) is hyperbolic if and only if $P'(\rho) > 0$, that is, the pressure must be a monotone increasing function of the mixture density ρ.

Let us denote by Ω ($\Omega \in \mathbb{R}^3$) the set of physical states

$$\Omega = \{\mathbb{U}(x,t) \in \mathbb{R}^3; \rho > 0, \alpha, c \in [0,1], u, u_r \in \mathbb{R}\},$$

then for $\mathbb{U} \in \Omega$ we can choose a number $\eta^\star$ such that for any $\mathbb{U}$ in the set $\Omega^\star$ defined as

$$\Omega^\star = \{\mathbb{U} \in \Omega : \rho(P) > 0, |\eta| \le \eta^\star\},$$

the eigenvalues λ_i, $1 \le i \le 3$ are real and distinct for η small enough and $\rho(P)$ satisfies (36). Thus, the eigenvalues of the matrix $\mathbb{A}(\mathbb{W})$ are the solutions of the characteristic equation

$$\det(\mathbb{A}(\mathbb{W}) - \lambda I) = 0.$$

Developing the determinant, we arrive to the general expression

$$\mathfrak{p}_0(\mathcal{X}) + \mathfrak{p}_1(\mathcal{X})\eta + \mathfrak{p}_2(\mathcal{X};\eta)\eta^2 = 0, \tag{37}$$

where

$$\begin{aligned}
\mathfrak{p}_0(\mathcal{X}) &= \mathcal{X}^3 - \mathcal{X},\\
\mathfrak{p}_1(\mathcal{X}) &= (1-2c)\mathcal{X}^2 - \left[1 - 2c - 2c(1-c)\rho\frac{\partial\psi}{\partial P}\right],\\
\mathfrak{p}_2(\mathcal{X};\eta) &= -\left\{\left[3c(1-c) + \rho(1-2c)a_m^2\frac{\partial c}{\partial P}\right]\mathcal{X}\right.\\
&\quad + \left[((1-2c)^2 + 2c(1-c))\rho a_m^2\frac{\partial c}{\partial P}\right.\\
&\quad \left.\left. + c(1-c)(1-2c)\right]\eta\right\},
\end{aligned}$$

and

$$\mathcal{X} = \frac{u-\lambda}{a_m}. \tag{38}$$

The roots of the characteristic Equation (37) for the model in general have not been found analytically. As shown by Toumi and Kumbaro (1996) and Zeidan *et al*. (2007a), we can find the eigenvalues according to the separated and mixture formulations of the flow in the one-dimensional space. Therefore, similar to the work developed by Zeidan *et al*. (2007a) for mixture formulations, the differential equations system (1)–(4) admits the following three eigenvalues

$$\lambda_i = \begin{cases} u - a_m + \mathcal{Y}u_r + \mathcal{O}(\eta^2) & i = 1,\\ u + [1 - 2c - 2\mathcal{Y}]u_r + \mathcal{O}(\eta^2) & i = 2,\\ u + a_m + \mathcal{Y}u_r + \mathcal{O}(\eta^2) & i = 3, \end{cases} \tag{39}$$

with

$$\mathcal{Y} = \rho c(1-c)\frac{\partial\psi}{\partial P}.$$

Further, the corresponding right eigenvectors follow by straightforward computation

$$\mathcal{K}^2 = \begin{pmatrix} -2\rho c(1-c)u_r \\ 0 \\ 1 \end{pmatrix}, \tag{40}$$

and

$$\mathcal{K}^{1,3} = \begin{pmatrix} \rho a_m \\ \pm 1 + \eta\mathcal{Y} \\ \pm\rho\frac{\partial\psi}{\partial P} + \rho\eta\frac{\partial\psi}{\partial P}\left(1 - 2c - \mathcal{Y} + \frac{1}{\rho}\frac{\partial P}{\partial\psi}\right) \end{pmatrix}. \tag{41}$$

Finally, we find that the first and third characteristic fields are genuinely non-linear and the second characteristic field is neither genuinely non-linear nor linearly degenerate as we shall see in the next section.

4. Nature of characteristic fields

In view of the hyperbolicity analysis demonstrated in the previous section, we study the nature of the characteristic fields of the model equations. From the eigenvalues (39), we obtain

$$\lim_{\eta\to 0}\nabla\lambda_1(\mathbb{U}) = \left[-\frac{\partial a_m}{\partial P}, 1, \mathcal{Y}\right],$$

$$\lim_{\eta\to 0}\nabla\lambda_3(\mathbb{U}) = \left[\frac{\partial a_m}{\partial P}, 1, \mathcal{Y}\right],$$

and

$$\lim_{\eta\to 0}\nabla\lambda_2(\mathbb{U}) = [0, 1, 1 - 2c - 2\mathcal{Y}].$$

From which we find for both the first and third eigenvalue–eigenvector pairs $(\lambda_1, \mathcal{K}^1)$ and $(\lambda_3, \mathcal{K}^3)$

$$\begin{aligned}
&\lim_{\eta\to 0}\nabla\lambda_1(\mathbb{U})\cdot\mathcal{K}^1(\mathbb{U})\\
&= -\frac{a_m^{-2}}{2}\left[2\frac{\partial P}{\partial\rho} + \rho\frac{\partial^2 P}{\partial\rho^2} + 2\mathcal{Y}\rho a_m^2\frac{\partial\psi}{\partial P}\right],
\end{aligned} \tag{42}$$

$$\begin{aligned}
&\lim_{\eta\to 0}\nabla\lambda_3(\mathbb{U})\cdot\mathcal{K}^3(\mathbb{U})\\
&= \frac{a_m^{-2}}{2}\left[2\frac{\partial P}{\partial\rho} + \rho\frac{\partial^2 P}{\partial\rho^2} + 2\mathcal{Y}\rho a_m^2\frac{\partial\psi}{\partial P}\right].
\end{aligned} \tag{43}$$

Using (35) and (36), we find that the first and the third characteristic fields are genuinely non-linear.

For the second characteristic field, we obtain

$$\lim_{\eta\to 0}\nabla\lambda_2(\mathbb{U})\cdot\mathcal{K}^2(\mathbb{U}) = 1 - 2c - 2\mathcal{Y}. \tag{44}$$

The expression in Equation (44) is positive for $c = 0$ and negative for $c = 1$, thus this field is neither genuinely non-linear nor linearly degenerate. Equation (14) together with the mixture density from system (18) and (20), (44) can be written as

$$\lim_{\eta\to 0}\nabla\lambda_2(\mathbb{U})\cdot\mathcal{K}^2(\mathbb{U}) = 1 - 2\alpha, \tag{45}$$

where $\alpha = \alpha_2$ is the volume fraction for the gas phase.

5. Numerical solution of the full two-phase flow equations

The numerical algorithm employed in this article for solving numerically the governing Equations (24)–(26) in the conservative form (27) is based on the methodology of finite volume methods for systems of hyperbolic conservation laws (Toro 2009). Integration of Equation (27) over a computational cell of length Δx_i and between times t^n and t^{n+1} yields

$$\mathbb{U}_i^{n+1} = \mathbb{U}_i^n - \frac{\Delta t}{\Delta x}\left[\mathbb{F}_{i+\frac{1}{2}} - \mathbb{F}_{i-\frac{1}{2}}\right] + \Delta t \mathbb{S}_i. \tag{46}$$

Here $\mathbb{U}_i^n$ is the average value of $\mathbb{U}$ over cell i at time level n. The time step Δt is calculated by

$$\Delta t = \mathrm{CFL}\ \frac{\Delta x}{S_{\max}^{(n)}}, \tag{47}$$

where CFL $\in [0, 1]$ is the Courant-Friedrichs-Lewy number and $S_{\max}^{(n)}$ is the maximum wave speed at the current time level chosen as

$$S_{\max}^{(n)} = \max_i \{|\lambda_i|\}, \tag{48}$$

where λ_i are eigenvalues corresponding to sound waves. $\mathbb{F}_{i+\frac{1}{2}}$and $\mathbb{F}_{i-\frac{1}{2}}$ are the numerical fluxes and $\mathbb{S}_i$ represents the numerical source terms. Very often, numerical approximations for systems of form (27) are accomplished by using a fractional splitting procedure (Strang 1968). In this approach, one alternate between solving the homogeneous system of conservation laws

$$\frac{\partial \mathbb{U}}{\partial t} + \frac{\partial \mathbb{F}(\mathbb{U})}{\partial x} = 0, \tag{49}$$

which is the source-free hyperbolic model and the non-homogeneous system of ordinary differential equations

$$\frac{d\mathbb{U}}{dt} = \mathbb{S}(\mathbb{U}). \tag{50}$$

Equation (50) is often solved with any classical numerical tool, such as the Runge–Kutta scheme, an explicit or implicit Euler scheme or any available scheme to obtain the complete solution of the system Equations (27).

The splitting technique requires that the homogeneous system (49) in which discontinuities are present be performed over the time step Δt and that the non-homogeneous problem in which phase-interaction occurs be performed over $\Delta t = t^{n+1} - t^n$. Because the system (27) is inhomogeneous, the numerical methods must be able to deal with shocks, contact discontinuities and rarefaction waves, and be capable of successfully incorporating the non-homogeneous terms. Thus, to approximate the solution of (27), we consider methods which are easily applicable to initial-boundary value problems with a large range of initial data and with shock-capturing, high order and total variation diminishing (TVD) capabilities. Accordingly, Godunov methods are considered for solving the homogeneous system (49). These methods are characterised as being of first-order or by their higher accuracy in the smooth regions of the solution without presenting the spurious oscillations associated with the conventional second-order methods in the presence of discontinuities. As our main focus is the demonstration of the proposed model, so we will consider Godunov methods of centred-type to approximate the numerical fluxes appearing in Equation (46). Godunov methods of centred-type are of great interest in numerous applications and have been widely used for single-phase and two-phase flows with varying degree of success (see e.g. Thevand *et al.* 1999, Romenski and Toro 2004, Zeidan *et al.* 2007b, Toro 2009). These methods do not explicitly require the condition of wave propagation information to be used in the numerical scheme apart from using stability constraints through a Courant-Friedrichs-Lewy (CFL) condition for which at least the eigenvalues of the system must be known. In the following, we give an outline of two general centred methods that can be easily and directly applied to the proposed model. The description below focuses on those aspects critical to the application and does not describe centred methods in any detail. For an in-depth and up-to-date description of these methods, refer to the recent textbook by Toro (2009).

A simple method for computing the numerical flux $\mathbb{F}_{i+\frac{1}{2}}$ is to use the first-order centred (FORCE) scheme (Chen and Toro 2004). The FORCE scheme is given by

$$\mathbb{F}_{i+\frac{1}{2}}^{\mathrm{FORCE}} = \frac{1}{2}\left(\mathbb{F}_{i+\frac{1}{2}}^{\mathrm{LF}} + \mathbb{F}_{i+\frac{1}{2}}^{\mathrm{RI}}\right), \tag{51}$$

where $\mathbb{F}_{i+\frac{1}{2}}^{\mathrm{LF}}$ is the Lax–Friedrichs flux

$$\mathbb{F}_{i+\frac{1}{2}}^{\mathrm{LF}} = \frac{1}{2}\left[\mathbb{F}(\mathbb{U}_i^n) + \mathbb{F}(\mathbb{U}_{i+1}^n)\right] + \frac{1}{2}\frac{\Delta x}{\Delta t}\left[\mathbb{U}_i^n - \mathbb{U}_{i+1}^n\right], \tag{52}$$

and $\mathbb{F}_{i+\frac{1}{2}}^{\mathrm{RI}}$ is the Richtmyer flux which is computed by first defining an intermediate data

$$\mathbb{U}_{i+\frac{1}{2}}^{\mathrm{RI}} = \frac{1}{2}\left(\mathbb{U}_i^n + \mathbb{U}_{i+1}^n\right) + \frac{1}{2}\frac{\Delta t}{\Delta x}\left[\mathbb{F}\left(\mathbb{U}_i^n\right) - \mathbb{F}(\mathbb{U}_{i+1}^n)\right], \tag{53}$$

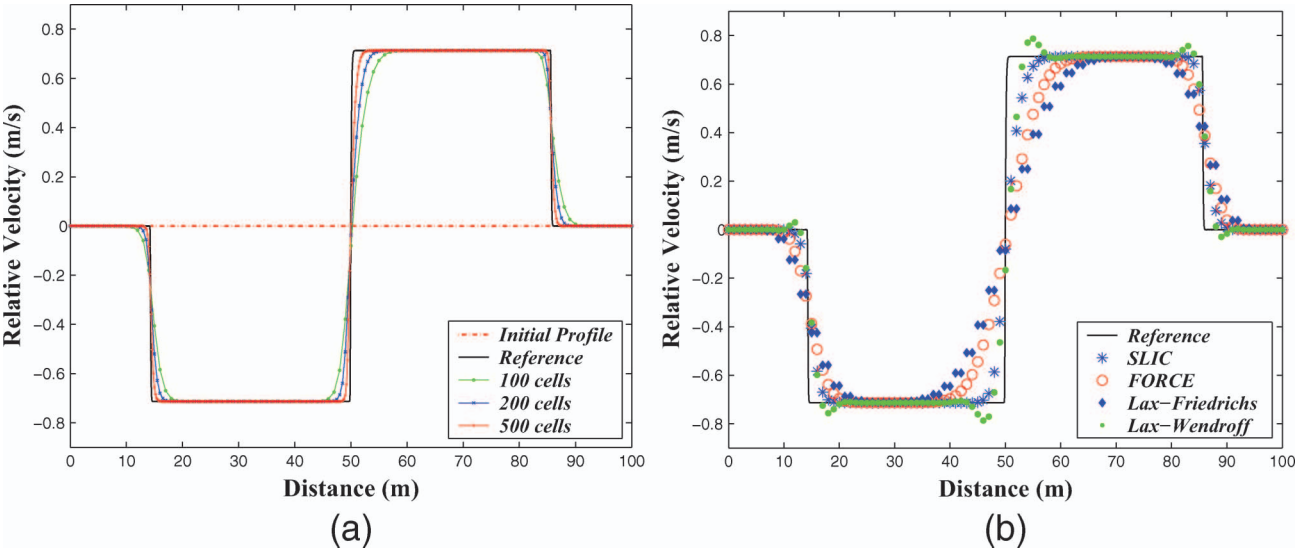

Figure 1. (a) Grid convergence study for the SLIC scheme with SUPERBEE limiter for the relative velocity profile when computing a standard shock tube problem at $t = 0.025$. The relative velocity vary through the middle wave associated to the eigenvalue λ_2. (b) Comparison of the predicted and reference solutions for the relative velocity profile at $t = 0.025$. A mesh of 100 cells is used for the numerical solutions using the Lax–Friedrichs, Lax–Wendroff, FORCE and TVD SLIC methods. The full black line is the reference solution and the symbols are the numerical solutions.

with

$$\mathbb{F}^{\mathrm{RI}}_{i+\frac{1}{2}} = \mathbb{F}\left(\mathbb{U}^{\mathrm{RI}}_{i+\frac{1}{2}}\right). \tag{54}$$

The FORCE scheme can be extended to a second-order non-oscillatory total variation diminishing, (TVD) slope limiter centred (SLIC) scheme (Toro and Billett 2000) following the MUSCL-Hancock approach (van Leer 1985). The first step in the SLIC scheme results in boundary extrapolated values

$$\mathbb{U}^L_i = \mathbb{U}^n_i - \frac{1}{2}\bar{\Delta}_i; \quad \mathbb{U}^R_i = \mathbb{U}^n_i + \frac{1}{2}\bar{\Delta}_i,$$

where $\bar{\Delta}_i$ is a limited slope to avoid spurious oscillation near large gradients of the solution and can be obtained using TVD constraints among the various limiters (Toro 2009). The boundary extrapolated values $\mathbb{U}^L_i, \mathbb{U}^R_i$ are then evolved in time by a half-time $\frac{1}{2}\Delta t$ as

$$\overline{\mathbb{U}}^{L,R}_i = \mathbb{U}^{L,R}_i + \frac{1}{2}\frac{\Delta t}{\Delta x}\left[\mathbb{F}\left(\mathbb{U}^L_i\right) - \mathbb{F}\left(\mathbb{U}^R_i\right)\right].$$

Finally, in order to advance the solution in time a Riemann problem is solved on each cell to obtain numerical flux contributions with the evolved data $\overline{\mathbb{U}}^{L,R}_i$ as

$$\mathbb{F}_{i+\frac{1}{2}} = \mathbb{F}_{i+\frac{1}{2}}\left(\overline{\mathbb{U}}^R_i, \overline{\mathbb{U}}^L_{i+1}\right), \tag{55}$$

using the FORCE flux as given by Equation (51).

6. Numerical results

In considering the performance of the proposed numerical methods, we will present numerical results from two test cases. The aim of these tests is to illustrate our proposed mathematical description of the model and to check the behaviour and accuracy of the numerical approach of the model equations. Also, to compare the numerical solutions obtained with the proposed model with an existing hyperbolic conservative two-phase flow model of a different type than currently used two-fluid models. Both tests consider an air–water mixture two-phase shock tube problem, the Riemann problem, with an appropriate initial and boundary conditions for each test case. This problem considers the homogeneous system only in Equation (27). The effect of the source terms is assessed afterwards. The first test consists of a Riemann problem for the model equations and deals with propagation of shock-waves in an air–water mixture two-phase flow. In the second test, we consider rarefaction-waves propagation within the mixture.

The shock tube, 100 m long, has a diaphragm in the middle to separate the left, $\mathbb{W}_L = [\rho_L, u_L, u_{rL}]$, and right, $\mathbb{W}_R = [\rho_R, u_R, u_{rR}]$, states. The numerical solutions are found with a coarse computational mesh of 100 cells at time $t = 0.025$ for shock-waves test problem and time $t = 0.007$ for the rarefaction-waves test problem. The CFL stability coefficient of 0.9 is used with transmissive boundary conditions. $S_{\max}$ is found using the simplified formula (48) and the SUPERBEE limiter was used to obtain second-order accuracy in

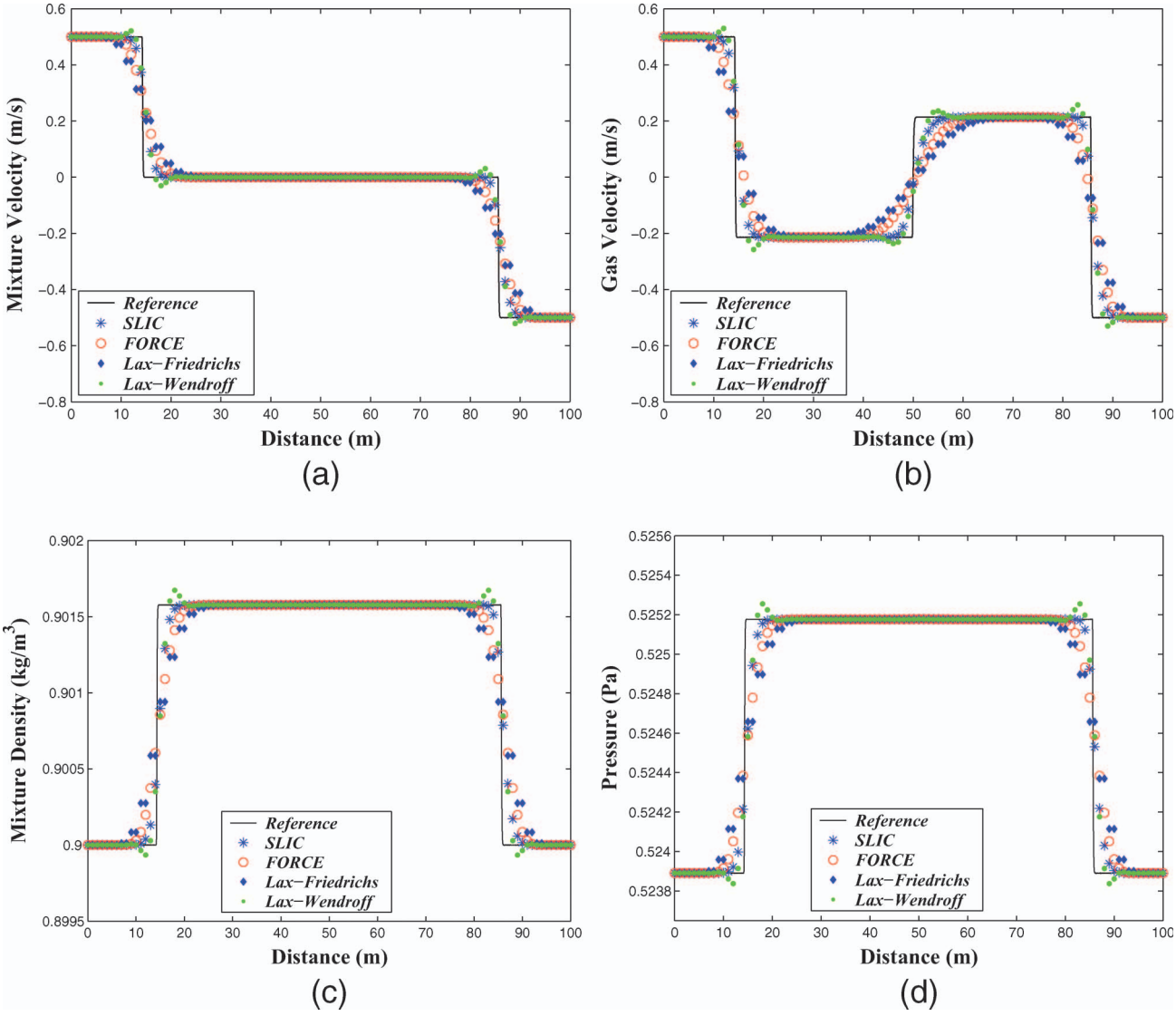

Figure 2. Numerical results for the mixture velocity, gas phase velocity, mixture density and pressure from four numerical methods (Lax–Wendroff, Lax–Friedrichs, FORCE and TVD SLIC) are compared with the reference solution at $t = 0.025$ on a mesh of 100 cells.

space. The SUPERBEE limiter has been our choice as it has shown a unique success in many practical computations, see for example Fraccarollo and Toro (1995), Romenski and Toro (2004), Zeidan *et al.* (2007b) and references there in. As there is no analytical solution to the model equations, the numerical results on a very fine computational mesh of 3000 cells (as meshes of a larger number of cells were checked to produce no further improvement) offers a guideline to the wave structure. However, for the states $\mathbb{W}_L$ and $\mathbb{W}_R$ we know that the solution is composed of three waves which are either shock, rarefaction or contact discontinuity separated by constant states. The numerical results for both tests will be compared with a reference numerical solution computed using the TVD SLIC scheme.

6.1. *Shock-waves propagation within an air–water mixture*

The initial states for the air–water mixture two-phase flow Riemann problem are given by $\mathbb{W}_L = [\rho_L,\ u_L,\ u_{rL}] = [0.9,\ 0.5,\ 0]$ and $\mathbb{W}_R = [\rho_R,\ u_R,\ u_{rR}] = [0.9,\ -0.5,\ 0]$. As we do not have an analytical solution to this Riemann problem, the numerical results on a very fine mesh provides a guideline to the wave structure which consist of two symmetric shock waves travelling in opposite directions separated by a middle wave as shown in Figure 1a. There are three wave families in Figure 1a. The outer waves correspond to the non-linear fields associated with the eigenvalues $\lambda_1 = u - a_m + \mathcal{Y}u_r$ and $\lambda_3 = u + a_m + \mathcal{Y}u_r$. The middle wave corresponds to neither genuinely non-linear nor

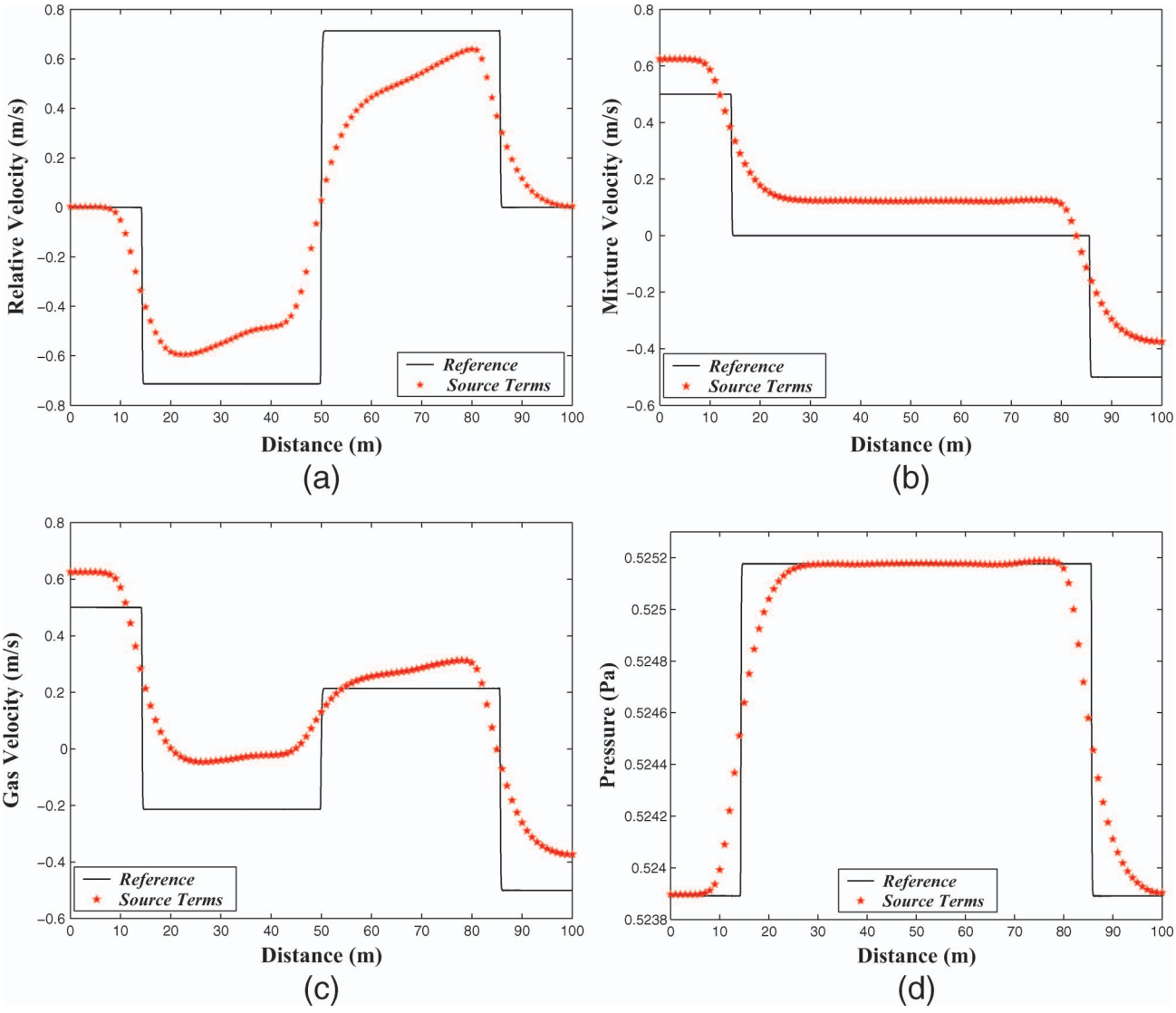

Figure 3. Effect of the source terms on the structure of shock-waves propagating in an air–water mixture two-phase flow at $t = 0.025$ with a mesh of 100 cells using the splitting procedure and the TVD SLIC scheme. The symbols represent the source terms effect and the solid line represents the reference solution. (a) Relative velocity, (b) mixture velocity, (c) gas velocity and (d) pressure.

linearly degenerate field associated with eigenvalue $\lambda_2 = u + [1 - 2c - 2\mathcal{Y}]u_r$ through which the relative velocity changes sign. Also, in Figure 1a we perform a grid convergence study for the relative velocity profile at time $t = 0.025$ using the TVD SLIC scheme for gradually finer meshes (a coarse mesh of 100 cells, a medium mesh of 200 cells and a fine mesh of 500 cells). Clearly, the results show that the waves take finer and finer structure as the number of cells is increased for computation. The reference solution was calculated by the TVD SLIC scheme using a mesh of 3000 cells. As it appears from this plot, the TVD SLIC scheme solutions are very satisfactory, oscillations-free and show convergence towards the reference solution.

Figure 1b shows a comparison of the relative velocity profile for the TVD SLIC, FORCE, Lax–Friedrichs and Lax–Wendroff methods at $t = 0.025$. Here, we see that the numerical solution of the TVD SLIC scheme remains in excellent agreement with the reference solution. In particular, the FORCE scheme produces practically identical results as the reference solution and smear discontinuities better than the Lax–Friedrichs and Lax–Wendroff methods. This is clearly seen by pairing of neighbouring values in the Lax–Friedrichs scheme and by overshoots and undershoots in the vicinity of discontinuities in the Lax–Wendroff scheme. Comparing the results of the SLIC scheme with those of the FORCE, Lax–Friedrichs and Lax–

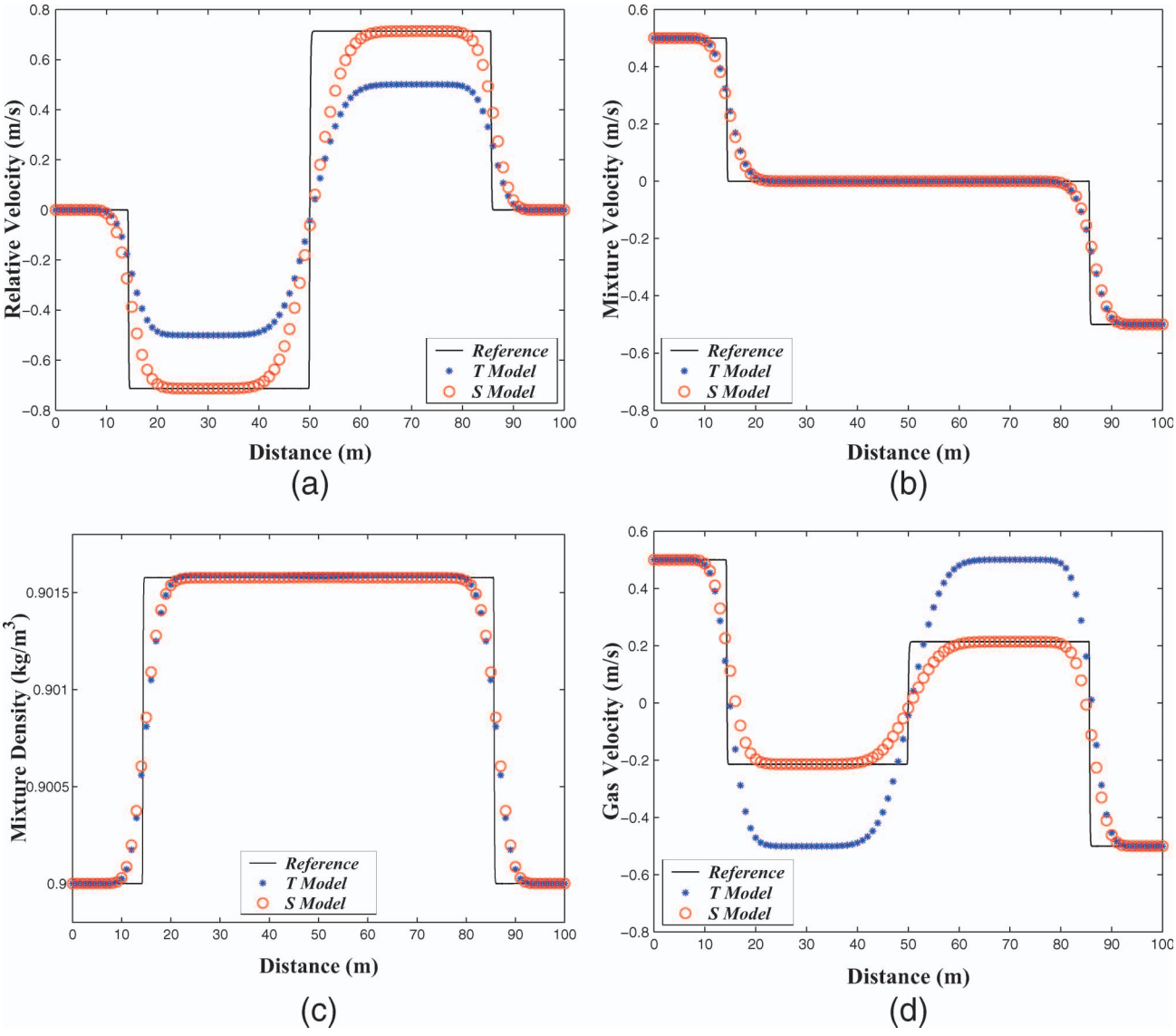

Figure 4. Results for shock waves test problem using the two different models (the S model and T model) together with the FORCE scheme at $t = 0.025$ with 100 mesh cells. The solid line represent the reference solution, (○) is the simple model and (*) is the thermodynamically compatible model. (a) Relative velocity, (b) mixture velocity, (c) mixture density and (d) gas velocity.

Wendroff methods we conclude that the TVD SLIC scheme produces oscillation-free results of improved quality to those from the first-order methods.

To illustrate the results provided by the proposed numerical methods, we display some physical variables (Figure 2a–d), namely, the mixture velocity, gas phase velocity, the mixture density and the pressure. Each plot shows the solutions at $t = 0.025$ and one observe that the four methods provide a similar resolution of the wave structure as the reference solution. Furthermore, we observe that the TVD SLIC scheme gives a sharp resolution of the discontinuities than the FORCE and Lax–Friedrichs methods and converges uniformly to the reference solution and no oscillations are visible. It is clear that the results of the Lax–Friedrichs scheme show their characteristic property of pairing cells values whereas the Lax–Wendroff scheme suffers from the numerical overshoots and undershoots in the approximation of all flow variables.

Having shown the convergence of the proposed numerical methods for the source-free hyperbolic model, we now turn our attention to the numerical solution of the full two-phase flow equations with the source terms using the full numerical methods of section 5. Figure 3a–d displays the relative velocity, mixture velocity, gas phase velocity and the pressure at $t = 0.025$ using the splitting procedure together with the TVD SLIC scheme. The symbols curves in each plot are obtained using the splitting approach and they represent the gravitational force appearing in the

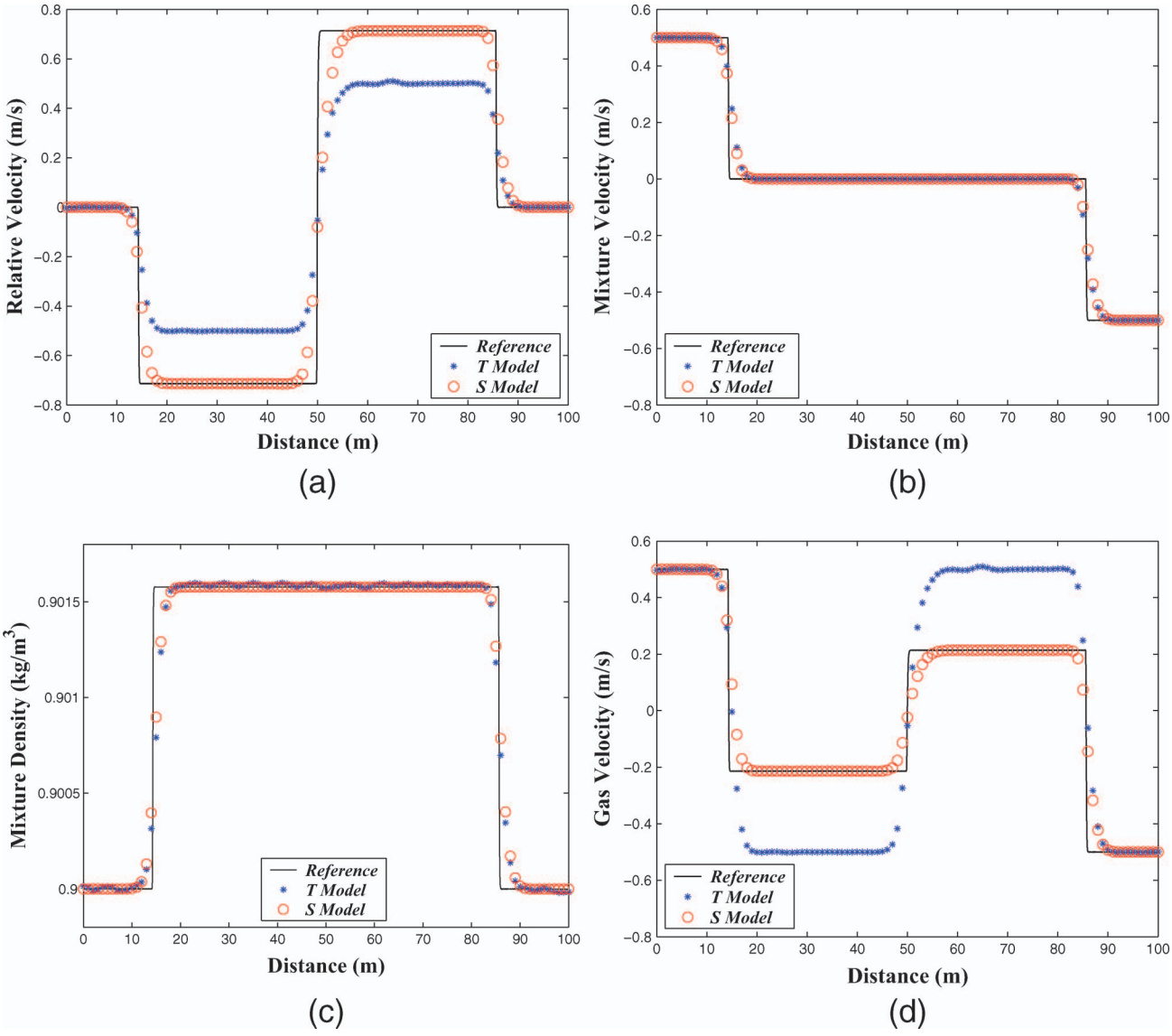

Figure 5. Results for shock-waves test problem using the S model, ○, and the T model, *, and the TVD SLIC scheme $t = 0.025$ on a mesh of 100 cells. The solid line represents the reference solution computed with the TVD SLIC scheme for 3000 mesh cells. (a) Relative velocity, (b) mixture velocity, (c) mixture density and (d) gas velocity.

mixture momentum Equation (25) and the drag force $\mathcal{S}^I$ in Equation (26) with κ defined as (Saurel and Lemetayer 2001, Zeidan *et al.* 2007b)

$$\kappa = \frac{1}{8} c(1-c) C_{\mathrm{D}} \frac{\rho^2}{\rho_2} |ur|, \tag{56}$$

where the drag coefficient $C_{\mathrm{D}} = 500$. From the plots, one can observe that the mixture velocity and gas phase velocity shows the upper discontinuities when the source terms are included. This is due to phase interaction as it passes through the Riemann problem structure. In particular, both the left and right propagating waves and the contact discontinuity have a continuous structure. The results shown here indicate that the momentum and relative velocity source terms have a strong effect on the proposed two-phase flow model.

A further test of the proposed numerical methods can be done by comparing the numerical results obtained with the model considered in this article with an existing two-phase flow model of a different type. Such a model based on the theory of thermodynamically compatible systems of conservation laws and formulated in terms of mixture parameters of state (Zeidan *et al.* 2007a). In all the following plots, we use S model and T model labels to refer to the simplest two-fluid model proposed in the current article and to

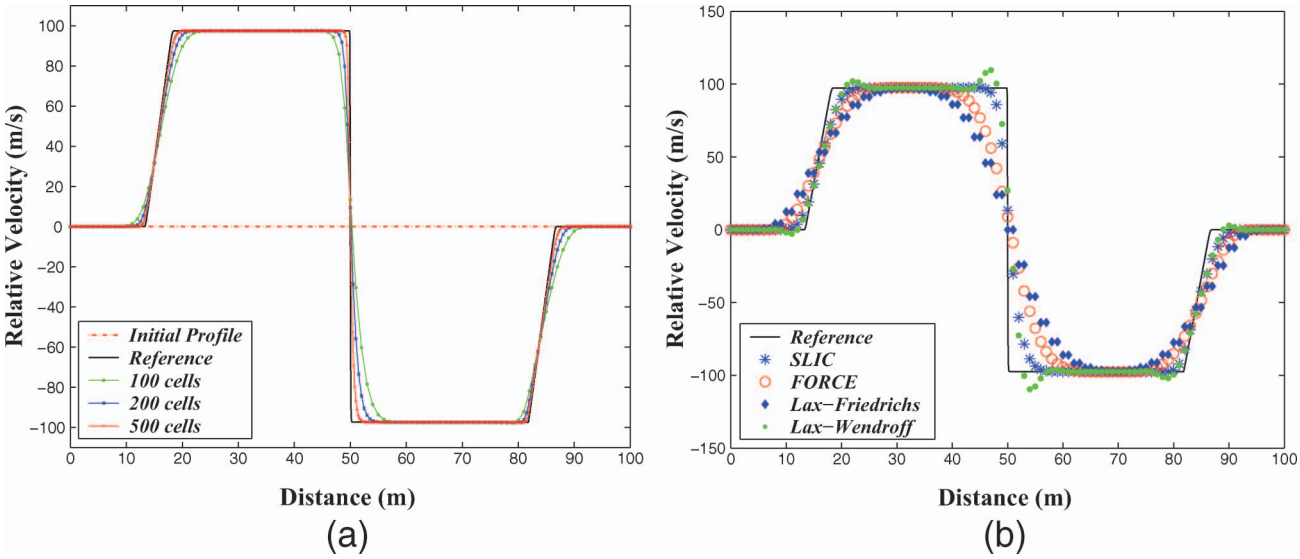

Figure 6. (a) Grid convergence of the relative velocity profile at time $t = 0.007$ for the SLIC scheme using the SUPERBEE limiter for two-rarefactions test problem. Numerical solutions with 100 (coarse), 200 (medium) and 500 (fine) mesh cells are shown. (b) Comparison of relative velocity between the reference and numerical solutions obtained using four numerical methods (the TVD SLIC, FORCE, Lax–Friedrichs and the Lax–Wendroff) at $t = 0.007$ with 100 cells. Reference solution shown by full line and the numerical solutions are displayed by symbols.

the thermodynamically compatible two-phase flow model, respectively. Figure 4a–d shows the results for the different models using the FORCE scheme at $t = 0.025$. From these figures, we can see that the very smooth distribution of the flow variables with both models and have the same behaviour. A numerical diffusion in the relative velocity and gas phase velocity profiles spread across the contact discontinuity is clearly visible with the T model. The reason for this behaviour in the T model is due to its mathematical structure as the model is highly non-linear with a different mathematical modelling approach. Both of the solutions of the FORCE scheme are oscillations-free and in excellent agreement with the reference solution.

Finally, Figure 5a–d displays our last check on the numerical results for different models using the TVD SLIC scheme at $t = 0.025$. Here, we note that both models have the same behaviour across the two shocks and the contact discontinuity, except the T model that gives a spread numerical diffusion in the relative velocity and gas phase velocity. Also evident from this figure a completely oscillations-free distribution for the S model across the contact discontinuity and shock waves. We also note that the solutions from the T model contain small kinks in all of the variables across the contact discontinuity. These kinks are referred to as 'start-up errors' and were first reported in (Woodward and Colella 1984). From this test problem, we conclude that the proposed numerical methods give essentially accurate and oscillations-free results for both models. This is due to the mathematically desirable features of both models as being hyperbolic and conservative.

6.2. *Rarefaction-waves propagation within an air–water mixture*

The tube in this test problem is filled with an air–water mixture two-phase flow with the left and right states defined as: $\mathbb{W}_L = [\rho_L,\ u_L,\ u_{rL}] = [800,\ -100,\ 0]$ and $\mathbb{W}_R = [\rho_R,\ u_R,\ u_{rR}] = [800,\ 100,\ 0]$. The results displayed are obtained using Godunov methods of centred-type with two different models at $t = 0.007$. These results then will be compared with the reference solution obtained using the TVD SLIC scheme with a very fine mesh. The accuracy of the reference solution is evaluated by conducting a grid convergence study. Figure 6a shows the convergence of the SLIC scheme together with the SUPERBEE limiter for various grid resolutions. For the calculations, we employ a coarse (100 cells), medium (200 cells) and fine (500 cells) meshes at $t = 0.007$. From the results plotted in Figure 6a, one can identify two symmetric rarefaction waves for the relative velocity, u_r, separated by a contact discontinuity. Also, one can note that the relative velocity changes discontinuously across λ_2. As it appears from this plot, various grid resolutions show the convergence of the method towards the reference solution. Figure 6b shows the comparison of the coarse mesh between the numerical results calculated with different methods and the reference solution for the

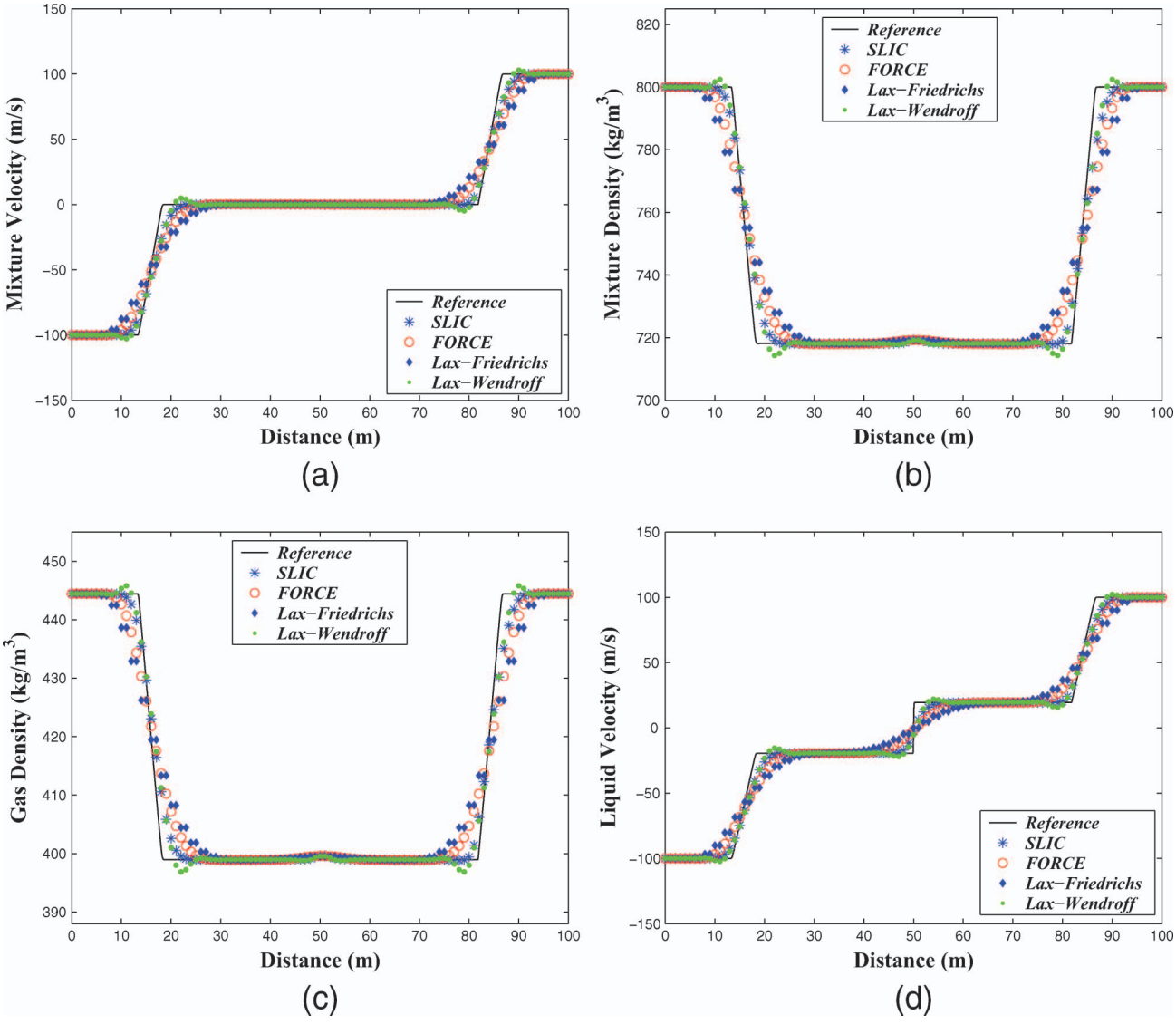

Figure 7. Numerical results for the mixture velocity, mixture density, gas density and liquid velocity from four numerical methods (TVD SLIC, FORCE, Lax–Friedrichs and Lax–Wendroff) are compared at $t = 0.007$ with the reference solution. The solid line shows the reference solution and the symbols show the numerical solutions.

relative velocity profile. In this plot, we note that the TVD SLIC give essentially oscillation-free results and well produce the reference solution. Particularly, both the head and the tail of the rarefaction waves accurately reproduced as sharp features. In addition, we observe no numerical oscillations in the results corresponding to the FORCE scheme. Also, one can see that the Lax–Friedrichs scheme shows their characteristic property of pairing cells values while visible undershoot and overshoot in the Lax–Wendroff scheme.

A closer look at the numerical solution at $t = 0.007$ is taken by displaying the profiles of the mixture velocity, mixture density, gas density and the liquid velocity. Figure 7a–d shows the major flow structure – left and right rarefactions separated by a contact discontinuity – are all noticeably better resolved and oscillation-free with the TVD SLIC scheme. In particular, we see that the solution of the FORCE scheme remains in excellent agreement with the reference solution. The solutions of the Lax–Friedrichs scheme, on the other hand, shows their property similar to those observed in Figure 6b. We also note that the solution from the Lax–Wendroff scheme suffer from undershoot and overshoot before and after the rarefaction waves. A very small kink in the mixture density and gas phase density is obtained in the vicinity of the contact discontinuity in all the four numerical methods is almost visible in Figure 7b and c. As in the previous test problem, these kinks are due to the start-up errors (Woodward and Colella 1984).

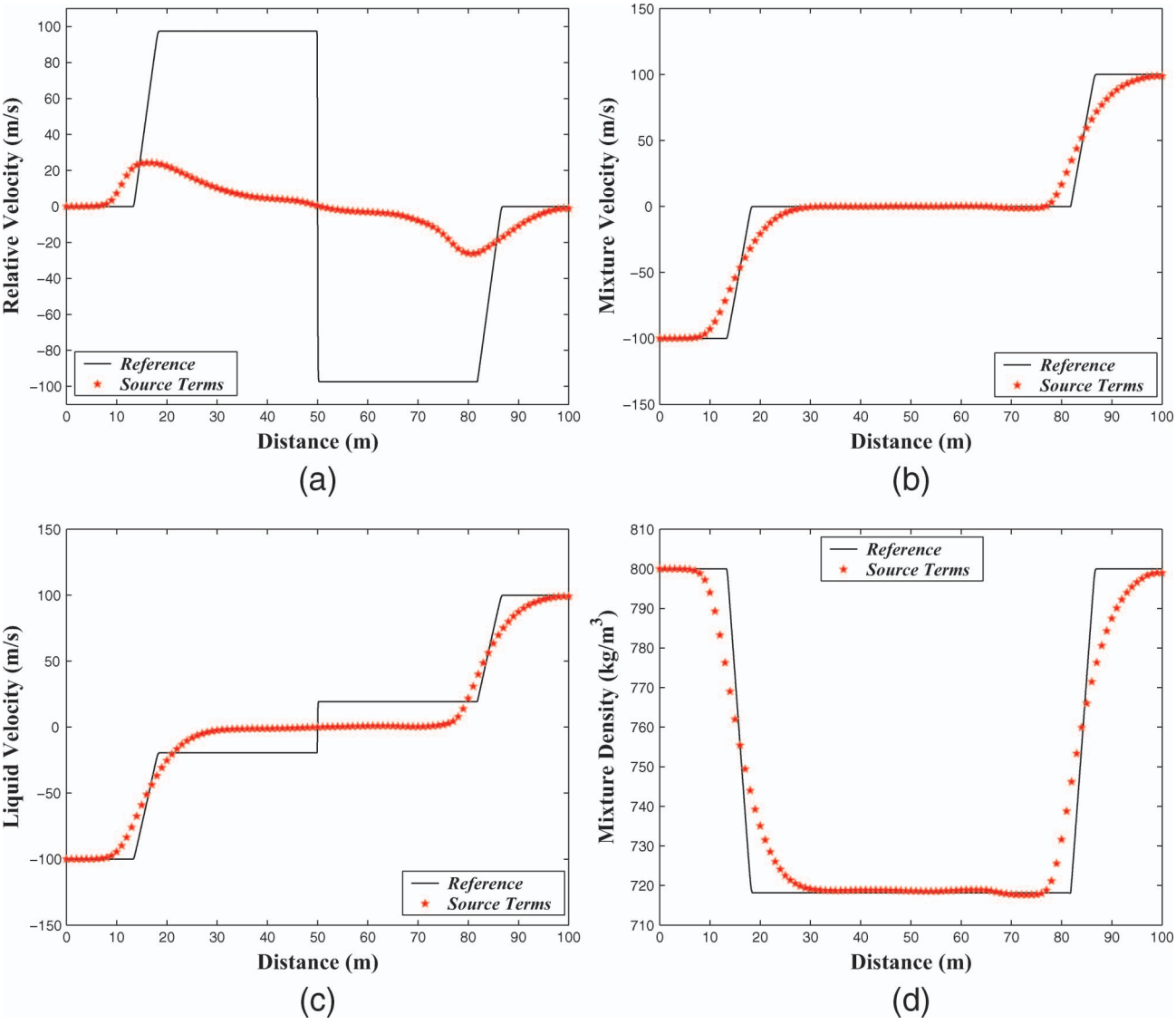

Figure 8. Numerical solution of the full two–phase flow equations using the splitting technique together with the TVD SLIC scheme on a mesh of 100 cells at $t = 0.007$. The source terms solutions are shown as symbols while the reference solution is shown as a solid line. (a) Relative velocity, (b) mixture velocity (d) liquid velocity and (d) mixture density.

Figure 8a–d displays the solution of the full two-phase flow equations. With the gravitational force source term in the mixture momentum Equation (25) and the drag force source term in Equation (26) included, phase interaction is predicted to occur immediately and flow variables decrease as it passes through the Riemann problem structure for which the left and right propagating waves and the contact discontinuity will have a continuous structure.

In order to test the performance of the proposed numerical methods in terms of both accuracy and robustness, we compare the numerical solutions in Figures 9a–d and 10a–d with solutions computed using the thermodynamically compatible two–phase flow model. As in the previous test we will use S model and T model labels to refer to the current model presented in this article and to the thermodynamically compatible model. Figure 9a–d shows the profiles of the relative velocity, mixture velocity, mixture density and the gas density at $t = 0.007$ using the FORCE scheme for the different models. A significant agreement on the behaviour is achieved. The solutions are completely oscillation-free and able to reproduce the head and the tail of the rarefaction waves for all the flow variables. From these plots one can see the small kinks in the mixture density and gas density results generated using the S model across the contact discontinuity. As already remarked, these are related to the start-up errors. Also, a very small dip in the mixture density and gas phase density is obtained in

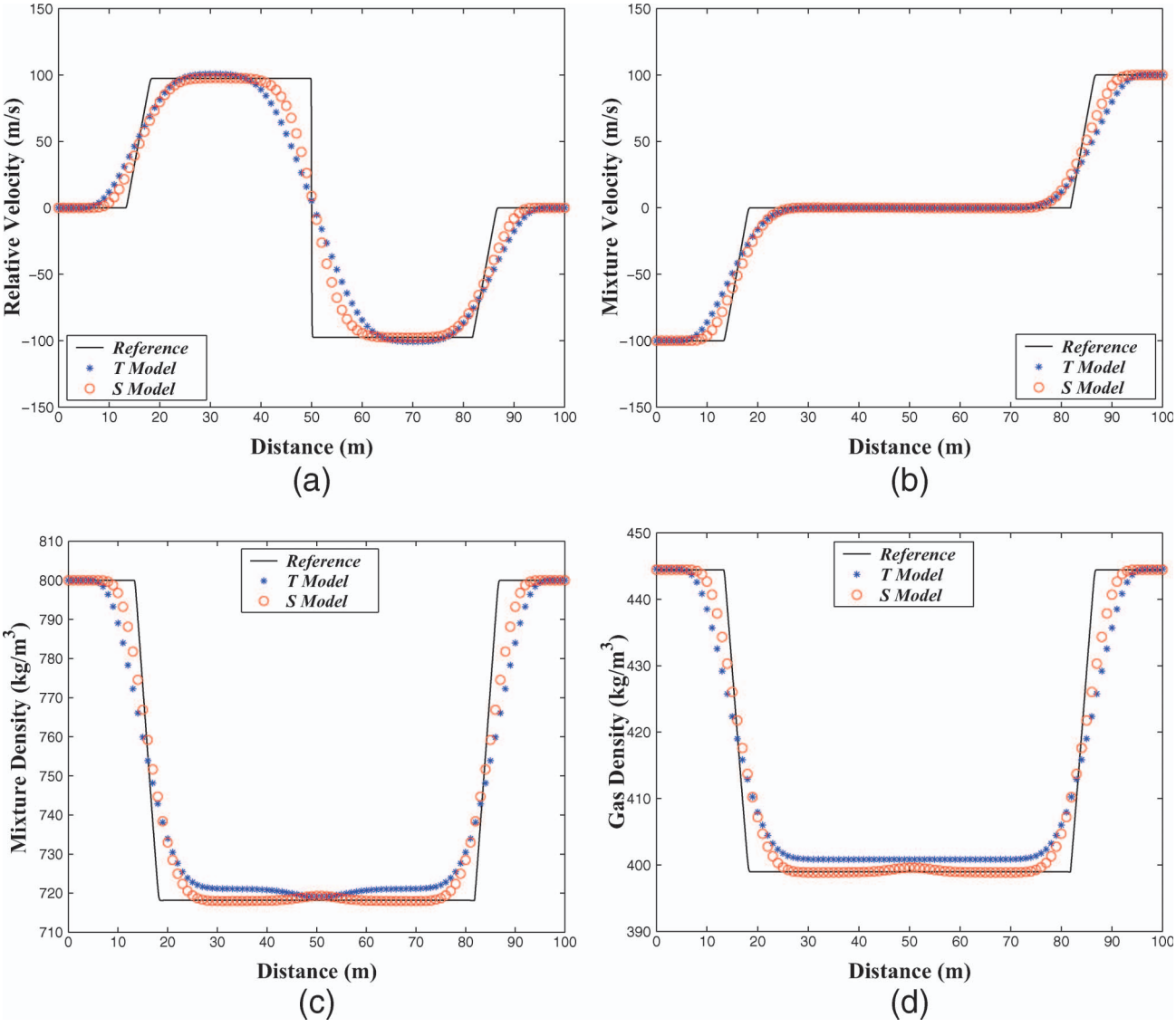

Figure 9. Comparison between the S model, ○, and the T model, *, for the two-rarefactions test problem using the FORCE scheme on a mesh of 100 cells at $t = 0.007$. (a) Relative velocity, (b) mixture velocity, (c) mixture density and (d) gas density.

the vicinity of the contact discontinuity in the T model is clearly visible in Figure 9c and d. This is due to spurious mixture density perturbations which are intrinsic anomalies of hyperbolic systems. Such anomalies are related to the selected two-phase flow equations but not to the selected numerical methods proposed in this article. Anomalies reported here were first noted for hyperbolic conservative models of two-phase flow problems in (Zeidan *et al.* 2007a). Furthermore, anomalies reported here do affect other hyperbolic systems such as artificial compressibility equations associated with steady incompressible Navier–Stokes equations, equations of magnetohydrodynamics and Euler equations (Toro 2002).

As a final calculation we compare the numerical solutions at $t = 0.007$ for the S model and the T model using the TVD SLIC scheme. Figure 10a–d shows the profiles of the relative velocity, mixture velocity, mixture density and the gas density, respectively, at $t = 0.007$. From these plots, we can observe that both models have the same behaviour. In particular, the numerical solution is very satisfactory and oscillations-free distribution for the flow variables are obtained with the TVD SLIC scheme. As it appears from these plots, no spurious oscillations of flow variables were obtained across the contact discontinuity using the TVD SLIC scheme with both models. Figure 10c and d shows a small kink in the mixture density and gas density across the contact discontinuity which is clearly visible with the S model. A small dip in the mixture density and gas density is also visible across the contact discontinuity with the T model. As noted previously,

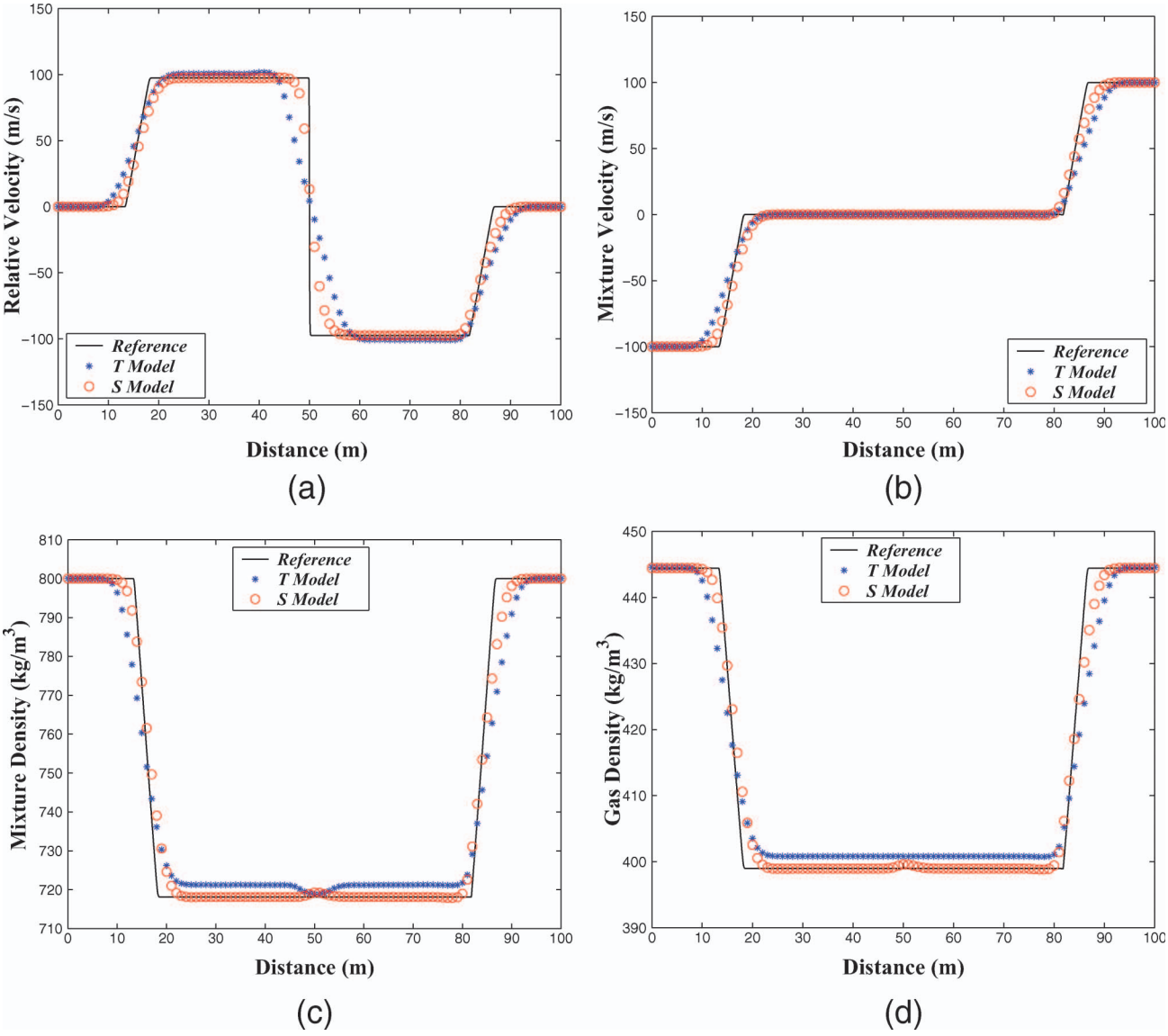

Figure 10. Numerical results for rarefaction waves test problem obtained using the two models and the TVD SLIC scheme at $t = 0.007$ on a mesh of 100 cells: black curves show the reference solution; ○, the S model; * the T model. (a) Relative velocity, (b) mixture velocity, (c) mixture density and (d) gas density.

the small kinks in the S model are referred to as start-up errors and the small dips in the T model are related to the anomalies of hyperbolic systems. We conclude from this test problem that the S model together with Godunov methods of centred-type gives essentially oscillation-free results for all flow variables.

7. Conclusions

We have demonstrated a methodology for examining the well-posedness of a two-fluid model of two-phase flows in a conservative from. The model is initially in a non-conservative form due to the presence of non-conservative products in the momentum equations. It is shown that the phase momentum equations can be written in a sum and a difference formulation in which the velocity of the two-phase mixture is given by the mixture momentum equation and in which the relative velocity between the phases can be expressed by a constitutive equation. The Jacobian matrix of the equation system model is derived and it is shown that the model is hyperbolic in a physically reasonable region of parameters; three real and distinct eigenvalues are obtained under the assumption that the relative velocity between the two phases is much lower than the speed of sound of the two-phase mixture. Also the corresponding eigenvectors for the system are determined and it is shown that the first and third

characteristic fields are genuinely non-linear while the second characteristic field is neither genuinely non-linear nor linearly degenerate.

On the basis of the conservative form and the hyperbolic character of the proposed two-phase flow equations, splitting techniques have been successfully implemented in an existing finite volume framework. Godunov methods of centred-type, originally developed for single-phase flow, were applied to the model equations and effectively used to capture discontinuous solutions. It is shown that the TVD SLIC scheme produces a very stable and accurate approximation for the solution of the homogeneous system of the model with the ability to capture discontinuities without spurious oscillations as demonstrated through the test problems presented in this article. For the complete solution of the model equations, where the source terms play a major role, the advantages of the TVD SLIC scheme are also evident, as illustrated by the preliminary results presented. Computed results obtained by the proposed methods are compared with different model equations available in the literature. The agreement is significant by the different models. From the comparison of the different models, the proposed methods do produce accurate and efficient solutions for modelling discontinuous solutions in two-phase flow problems.

The present findings call for further work on the numerical methods, investigation of more complex solutions in one and multiple dimensions, and improvements in the model for gas–liquid mixture flows, such as the incorporation of the energy equations. These paths are the subject of ongoing work and will be reported in forthcoming articles.

References

Baer, M. and Nunziato, J., 1986. A two-phase mixture theory for the deflagration-to-detonation transition (DDT) in reactive granular materials. *International Journal of Multiphase Flow*, 12, 861–889.

Barre, F. and Bernard, M., 1990. The CATHARE code strategy and assessment. *Nuclear Engineering and Design*, 124, 257–284.

Baudin, M., *et al*., 2005. A relaxation method for two-phase flow models with hydrodynamic closure law. *Numerische Mathematik*, 99, 411–440.

Bdzil, J.B., *et al*., 1999. Two-phase modelling of deflagration-to-detonation transition in granular materials: a critical examination of modelling issues. *Physics of Fluids*, 11, 378–402.

Bendiksen, K.H., *et al*., 1991. The dynamic two-fluid model OLGA: theory and application. *SPE Production Engineering*, 6, 171–180.

Brennen, C.E., 2005. *Fundamentals of multiphase flow*. Cambridge: Cambridge University Press.

Castro, C.E. and Toro, E.F., 2006. A Riemann solver and upwind methods for a two-phase flow model in non-conservative form. *International Journal of Numerical Methods in Fluids*, 50, 275–307.

Chen, G.Q. and Toro, E.F., 2004. Centred schemes for non-linear hyperbolic equations. *Journal of Hyperbolic Differential Equations*, 1, 531–566.

Chung, M.S., Chang, K.S., and Lee, S.J., 2002. Numerical solution of hyperbolic two-fluid two-phase flow model with non-reflecting boundary conditions. *International Journal of Engineering Science*, 40, 789–803.

Collela, P. and Woodward, P.R., 1984. The piecewise parabolic method (PPM) for gas-dynamical simulations. *Journal of Computational Physics*, 54, 174–201.

Coquel, F., *et al*., 1997. A numerical method using upwind schemes for the resolution of two-phase flows. *Journal of Computational Physics*, 136, 272–288.

Delhaye, J.M. and Achard, J.L., 1976. On the averaging operators introduced in two-phase flow modelling. *In*: *Proceedings of CSNI Specialist Meeting in Transient Two-Phase Flow*, Vol. 1. Toronto: Atomic Energy of Canada Ltd, 5–84.

Drew, D., Cheng, L., and Lahey, R.T., 1979. The analysis of virtual mass effects in two-phase flow. *International Journal of Multiphase Flow*, 5, 233–242.

Drew, D., 1983. Mathematical modelling of two-phase flow. *Annual Review of Fluid Mechanics*, 15, 261–291.

Drew, D. and Passman, S., 1998. *Theory of multicomponent fluids, (Applied mathematical Sciences, Vol. 135)*. New York: Springer-Verlag.

Fraccarollo, L. and Toro, E.F., 1995. Experimental and numerical assessment of the shallow water model for two-dimensional dam-break type problems. *Journal of Hydraulic Research*, 33, 843–864.

Garcia-Cascales, J.R. and Corberin-Salvador, J.M., 2006. Extension of a high-resolution scheme to 1D liquid–gas flow. *International Journal of Numerical Methods in Fluids*, 50, 1063–1084.

Godunov, S.K. and Romenskii, E., 2003. *Elements of continuum mechanics and conservation laws*. New York: Kluwer Academic/Plenum.

Gouin, H. and Gavrilyuk, S., 1999. Hamilton's principle and Rankine-Hugoniot conditions for general motions of mixtures. *Meccanica*, 34, 39–47.

Harten, A., 1989. ENO schemes with subcell resolution. *Journal Computational Physics*, 83, 148–184.

Ishii, M., 1975. *Thermo-fluid dynamic theory of two-phase flow*. Paris: Eyrolles.

Ishii, M. and Zuber, N., 1979. Relative motion and interfacial drag coefficient in dispersed two-phase flow of bubbles, drops and particles. *AIChE Journal*, 25, 843–855.

Lahey, R.T. Jr. and Drew, D.A., 1988. The three-dimensional time and volume averaged conservation equations of two-phase flows. *Advanced Nuclear Science and Technology*, 20, 1–69.

Larsen, M., *et al*., 1997. Petra: a novel computer code for simulation of slug flow. *In*: *SPE Annual Technical Conference and Exhibition, SPE 38841*, October, San Antonio, TX, 1–12.

Lee, S.J., *et al*., 1998. Surface tension effect in the two-fluids equations system. *International Journal of Heat Mass Transfer*, 41, 2821–2826.

Masella, J.M., Faille, I., and Gallouet, T., 1999. On an approximate Godunov scheme. *International Journal of Computatonal Fluid Dynamics*, 12, 133–149.

Nigmatulin, R.I., 1979. Spatial averaging in the mechanics of heterogeneous and dispersed systems. *International Journal of Multiphase Flow*, 5, 353–385.

Niu, Y.Y., 2001. Advection upwinding splitting method to solve a compressible two-fluid model. *International Journal of Numerical Methods in Fluids*, 36, 351–371.

Paillere, H., Corre, C., and Garcia Cascales, J.R., 2003. On the extension of the AUSM+scheme to compressible two-fluid models. *Computational Fluids*, 32, 891–916.

Papalexandris, M.V., 2004. Numerical simulation of detonations in mixtures of gases and solid particles. *Journal of Fluid Mechanics*, 507, 95–142.

Ren, Y.X., *et al*., 1996. A high order accurate, non-oscillating finite volume scheme using spline interpolation for solving hyperbolic conservation laws. *Acta Aerodynamica Sinica*, 14, 281–287.

Romate, J.E., 1998. An approximate Riemann solver for a two-phase flow model with numerically given slip relation. *Computational Fluids*, 27, 455–477.

Romenski, E. and Toro, E.F., 2004. Compressible two-phase flow models: two-pressure models and numerical methods. *Computational Fluid Dynamics Journal*, 13, 403–416.

Romenski, E., Resnyansky, D., and Toro, E.F., 2007. Conservative hyperbolic formulation for compressible two-phase flow with different phase pressures and temperatures. *Quarterly of Applied Mathematics*, 65, 259–279.

Saurel, R. and Lemetayer, O., 2001. A multiphase model for compressible flows with interfaces, shocks, detonation waves and shocks, detonation waves and cavitation. *Journal of Fluid Mechanics*, 431, 239–271.

Serre, D., 1993. On the variational principle for the equations of perfect fluid dynamics. *Modélisation mathématique et analyse numérique*, 27, 739–758.

Sha, W.T. and Soo, S.L., 1979. On the effect of $P\nabla\alpha$ term in multiphase mechanics. *International Journal of Multiphase Flow*, 5, 153–158.

Shieh, L.A.S., Krishnamurthy, R., and Ransom, V.H., 1994. Stability, accuracy, and convergence of the numerical methods in RELAP5/MOD3. *Nuclear Science Engineering*, 116, 227–244.

Stadtke, H., 2006. *Gasdynamic aspects of two-phase flow: hyperbolicity, wave propagation phenomena, and related numerical methods*. Weinheim: Wiley-VCH.

Stewart, H.B. and Wendroff, B., 1984. Two-phase flow: models and methods. *Journal of Computational Physics*, 56, 363–409.

Strang, G., 1968. On the construction and comparison of difference schemes. *SIAM Journal on Numerical Analysis*, 5, 506–517.

Stuhmiller, J.H., 1977. The influence of interfacial pressure forces on the character of two-phase flow model equations. *International Journal of Multiphase Flow*, 3, 551–560.

Thevand, N., Daniel, E., and Loraud, J.C., 1999. On high-resolution schemes for solving unsteady compressible two-phase dilute viscous flows. *International Journal of Numerical Methods in Fluids*, 31, 681–702.

Thomas, P.D. and Lombard, C.K., 1979. Geometric conservation law and its application to flow computations on moving grids. *AIAA Journal*, 17, 1030–1037.

Tiselj, I. and Petelin, S., 1997. Modelling of two-phase flow with second-order accurate scheme. *Journal of Computational Physics*, 136, 503–521.

Toro, E.F., 2009. *Riemann solvers and numerical methods for fluid dynamics. A practical introduction*. Berlin, Heidelberg: Springer-Verlag.

Toro, E.F. and Billett, S., 2000. Centred TVD schemes for hyperbolic conservation laws. *IMA Journal of Numerical Analysis*, 20, 47–79.

Toro, E.F., 2002. Anomalies of conservative methods: analysis, numerical evidence and possible cures. *Computational Fluid Dynamics Journal*, 11, 128–143.

Toumi, I. and Kumbaro, A., 1996. An approximate linearized Riemann solver for a two-fluid model. *Journal of Computational Physics*, 124, 286–303.

Toumi, I., 1996. An upwind numerical method for two-fluid two-phase flow models. *Nuclear Science Engineering*, 123, 147–168.

van Leer, B., 1985. On the relation between the upwind-differencing schemes of Godunov, Enguist-Osher and Roe. *SIAM Journal of Scientific and Statistical Computing*, 5, 1–20.

Woodward, P. and Colella, P., 1984. The numerical simulation of two-dimensional fluid flow with strong shocks. *Journal of Computational Physics*, 54, 115–173.

Zeidan, D., 2005. Numerical modelling of the Riemann problem for a mathematical two-phase flow model. *WIT Transactions on Engineering Sciences*, 50, 53–61.

Zeidan, D., *et al*., 2007a. Numerical study of wave propagation in compressible two-phase flow. *International Journal of Numerical Methods in Fluids*, 54, 393–417.

Zeidan, D., *et al*., 2007b. Numerical solution for hyperbolic conservative two-phase flow equations. *International Journal of Computational Methods*, 4, 299–333.